3-2014

Van Allen Probes observations of direct wave-particle interactions

Joseph F. Fennell
Aerospace Corporation

J. Roeder
Aerospace Corporation

W. S. Kurth
University of Iowa

M. G. Henderson
Los Alamos National Laboratory

B. A. Larsen
Los Alamos National Laboratory

See next page for additional authors

Recommended Citation

Fennell, J. F., et al. (2014), Van Allen Probes observations of direct wave-particle interactions, Geophys. Res. Lett., 41, 1869–1875, doi:10.1002/2013GL059165.

AGU PUBLICATIONS

Geophysical Research Letters

RESEARCH LETTER
10.1002/2013GL059165

Special Section:
Early Results from the Van Allen Probes

Van Allen Probes observations of direct wave-particle interactions

J. F. Fennell[1], J. L. Roeder[1], W. S. Kurth[2], M. G. Henderson[3], B. A. Larsen[3], G. Hospodarsky[2], J. R. Wygant[4], J. S. G. Claudepierre[1], J. B. Blake[1], H. E. Spence[5], J. H. Clemmons[1], H. O. Funsten[3], C. A. Kletzing[2], and G. D. Reeves[3]

[1]Space Science Applications Laboratory, Aerospace Corporation, El Segundo, California, USA, [2]Department of Physics and Astronomy, University of Iowa, Iowa City, Iowa, USA, [3]ISR Space Science and Applications, Los Alamos National Laboratory, Los Alamos, New Mexico, USA, [4]School of Physics and Astronomy, University of Minnesota, Minneapolis, Minnesota, USA, [5]Institute for the Study of Earth, Oceans, and Space, University of New Hampshire, Durham, New Hampshire, USA

Abstract Quasiperiodic increases, or "bursts," of 17–26 keV electron fluxes in conjunction with chorus wave bursts were observed following a plasma injection on 13 January 2013. The pitch angle distributions changed during the burst events, evolving from $\sin^N(\alpha)$ to distributions that formed maxima at $\alpha = 75$–80°, while fluxes at 90° and <60° remained nearly unchanged. The observations occurred outside of the plasmasphere in the postmidnight region and were observed by both Van Allen Probes. Density, cyclotron frequency, and pitch angle of the peak flux were used to estimate resonant electron energy. The result of ~15–35 keV is consistent with the energies of the electrons showing the flux enhancements and corresponds to electrons in and above the steep flux gradient that signals the presence of an Alfvén boundary in the plasma. The cause of the quasiperiodic nature (on the order of a few minutes) of the bursts is not understood at this time.

Key Points:
- Quasi-periodic bursts of electrons and chorus waves are simultaneous
- Electron angular distributions change dramatically during the bursts
- Burst electron energies are consistent with wave resonance conditions

Supporting Information:
- Readme
- Figure S1
- Figure S2
- Figure S3
- Figure S4
- Figure S5
- Figure S6

Correspondence to:
J. F. Fennell,
joseph.fennell@aero.org

Citation:
Fennell, J. F., et al. (2014), Van Allen Probes observations of direct wave-particle interactions, *Geophys. Res. Lett.*, *41*, 1869–1875, doi:10.1002/2013GL059165.

Received 1 JAN 2014
Accepted 19 FEB 2014
Accepted article online 23 FEB 2014
Published online 31 MAR 2014

1. Introduction

One of the more difficult observations to make in space plasmas is a direct confirmation of interaction between waves and electrons. Normally, the observed electron distributions do not show obvious features of the interactions that one can point to with certainty as either being caused by or being the source of the waves. In general, one observes only the resulting modified distributions. In this paper, we show a set of observations of isolated bursts of chorus waves along with simultaneous enhancements or bursts of electron fluxes that are constrained to a small range of particle pitch angles and energies.

The two Van Allen Probes (A and B) were launched in late August 2012 into nearly identical orbits [*Mauk et al.*, 2013]. Both satellites carry identical state of the art complements of particle and field measurements into ~600 by 30,500 km orbits with ~10° inclination. At the time of the observations presented, the apogees of the satellites were in the postmidnight region near 3 magnetic local time (MLT). They were relatively close together (see supporting information) with Probe B closer to apogee and leading Probe A by ~0.05 to 0.15 R_E in L-value [*McIlwain*, 1961] and separated by ~0.3 h in MLT. Both satellites were close to the magnetic equator, with B/B_0 ranging from ~1.006 to 1.004 for Probe A and from ~1.003 to 1.001 for Probe B, based on the *Tsyganenko* [1989] field model with $Kp = 2$, where B/B_0 is the ratio of the magnetic field intensity at the spacecraft to that at the magnetic equator.

2. Measurements Used

The particle measurements were made by the low-energy Magnetic Electron Ion Spectrometer (MagEIS) sensors [*Blake et al.*, 2013] that measure electrons in the ~20–240 keV energy range (hereafter designated as "LOW") and the Helium, Oxygen, Proton, and Electron (HOPE) [*Funsten et al.*, 2013] plasma sensors that cover the energy range from a few eV to ~50 keV. Both sensors are part of the Energetic Particle, Composition, and Thermal Plasma (ECT) particle suite [*Spence et al.*, 2013]. The wave observations were made by the Electric and Magnetic Field Instrument Suite and Integrated Science (EMFISIS) search coil sensors [*Kletzing et al.*, 2013] and the Electric Field and Wave sensors (EFW) [*Wygant et al.*, 2013]. EMFISIS was occasionally taking very high rate waveform data in its "burst mode" (BM). In BM, EMFISIS takes about 200,000 data points in a 6 s burst. The MagEIS LOW sensors were in their high-rate (HR) mode to support the ongoing Balloon Array for Radiation Belt

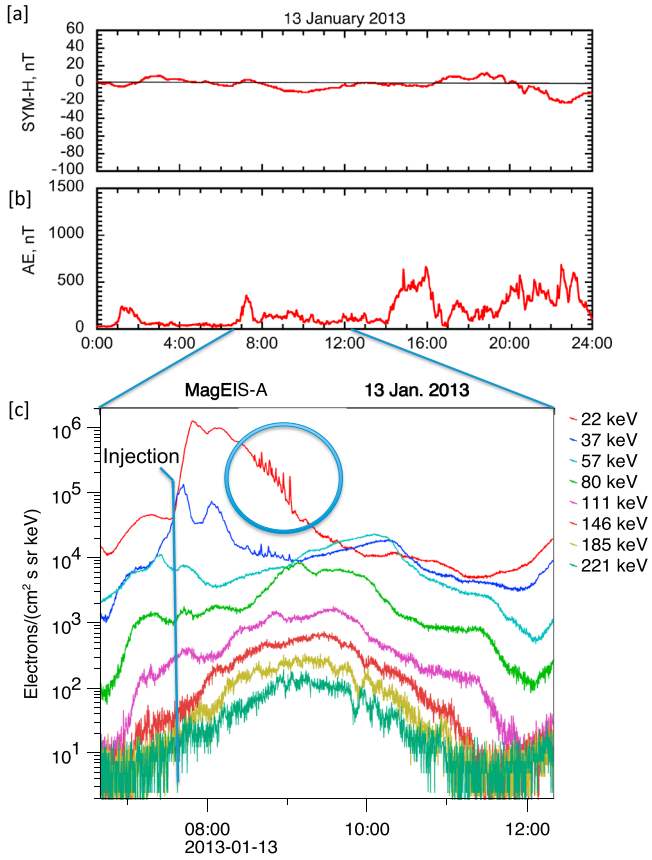

Figure 1. (a) *SYM-H* for January 2013, (b) *AE* for 13 January 2013, and (c) MagEIS-A electron fluxes from selected channels for one orbit on the 13 January. The period of interest is highlighted by the blue circle.

Relativistic Electron Losses (BARREL) campaign [*Millan et al.*, 2011]. In HR mode the MagEIS LOW sensors measured electron fluxes every ~10 ms in three broad electron energy ranges (HR0 ~ 20–40, HR1 ~ 40–91, and HR2 ~ 93–246 keV). In addition, the MagEIS LOW sensors took data in eight narrower energy channels at ~400 ms resolution. The HOPE sensor measured the full plasma electron and ion distributions on alternate ~10 s intervals. For this study we used HOPE electron data taken within ~18° of the satellite's spin/antispin axis directions. The MagEIS LOW sensor field of view is aligned at 105° relative to the spin axis, covering nearly a full range of angles relative to B during a satellite rotation. For the probes' nominal spin period of 10.5 s, a HR sampling interval corresponds to a rotation angle of ~0.34°.

3. Observations

Figure 1 provides an overview of the conditions. Figure 1a shows *SYM-H*, and Figure 1b shows *AE* for 13 January. *AE* was relatively quiet between 0400 and 1400 UT except for a <360 nT increase that started near 0730 UT. Figure 1c shows an overview of the electron fluxes observed by MagEIS on Van Allen Probe A (hereafter called A) as a series of line plots of the spin-averaged electron flux history for a selected set of energy channels (identified in the right-hand legend). A dispersive injection signature was observed starting near 0730 UT by MagEIS-A. (A similar signature was observed by B; see supporting information.). The electron injection onset is consistent with the *AE* increase in Figure 1b. The period of interest is where MagEIS-A observed bursts of low-energy electron flux increases identified by the circled region near the center of Figure 1c. These occurred as probe A approached apogee. Note that these flux bursts occurred only in the lowest energy MagEIS-A channels and during the decay of the substorm-injected electron fluxes back toward presubstorm levels.

The interval of electron flux bursts is expanded in Figure 2, which shows both a pitch angle versus time spectrogram of ~20–40 keV electrons in Figure 2a and a frequency-time spectrogram of whistler mode chorus bursts, taken by EMFISIS, in Figure 2b. Vertical dash-dotted white lines have been drawn through the flux bursts and extended through the wave spectrogram to highlight the strong correlation between the flux bursts and chorus bursts in the period of interest. These were nearly one to one. The spacing of the bursts was not periodic but is reminiscent of ultralow frequency oscillation periods in the Pc4/Pc5 range. However, no pulsations were observed in either Probe A or Probe B magnetic field or electric field measurements (not shown) (nor in GOES 13 and GOES 15 magnetometer data that were taken close in local time to the probes).

The electron pitch angle distributions in Figure 2a were measured by MagEIS-A LOW HR0 (~20–40 keV). These data show that the electron fluxes were most intense at pitch angles away from 90°, peaking instead from 75° to 80° (and 100°–105°). The pitch angle of peak flux varied slightly from flux burst to flux burst in the range 75–80° (100–105°, etc.). Given that these angular distributions are constrained to the electron energies measured by HR0 (and to >16 to <30 keV electrons measured by HOPE; see supporting information), this bears a resemblance to a ring distribution in velocity space. The angular peaks had full width at half maxima

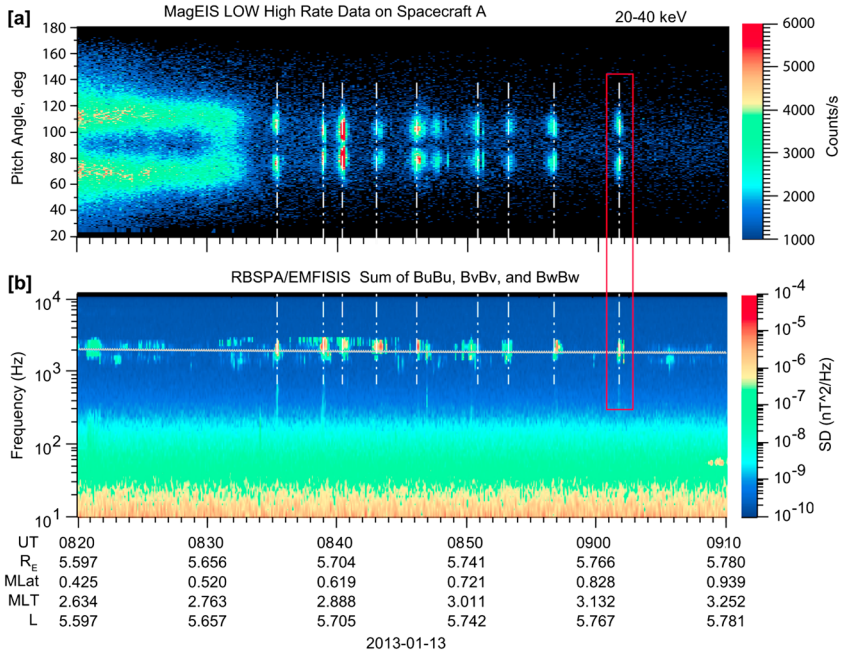

Figure 2. Comparison of electron flux bursts and chorus waves on 13 January 2013 during the 0820–0910 UT period. (a) A pitch angle spectrogram of 20–40 keV electrons with flux intensification bursts highlighted with vertical dash-dotted lines. (b) A frequency-time spectrogram from EMFISIS showing bursts of chorus emissions. The gray horizontal line demarks half the electron cyclotron frequency.

(FWHM) of order 18° ± 4. The narrow angular peaks of these burst fluxes were not resolvable using normal mode data. We also note that there were electron distributions with off 90° peaks from 0820 to 0833 UT when little or no chorus was present. We do not show the details of these distributions since we are focusing on the isolated flux and chorus bursts in the 0835–0905 UT range for this paper. However, we do note that the earlier off 90° angular peaks had FWHM at least twice those of the isolated bursts, indicating that they were probably formed some time previously and had dispersedly evolved, whereas, the isolated narrower bursts were most likely more recently generated.

A red box is drawn around the 0900:37–0902:15 UT interval in Figure 2 where EMFISIS took BM data during an electron flux burst. Figure 3 shows a succession of detailed pitch angle distributions taken by MagEIS-A HR0 during this interval. Figure 3a shows an example of a preburst pitch angle distribution that has been fitted with a function of form a $\sin^N(\alpha)$ where, in this case, $N \sim 0.8$ (note that Figure 3a covers angles of 0° to 180° only). Figures 3b–3j show the evolution of the pitch angle distributions through a flux burst. Each of Figures 3b–3j shows data for one satellite rotation with the angles of 0–180° being from the first half of a rotation and 180–0° being from the second half. This allows one to observe the pitch angle distribution changes half spin by half spin, i.e., with a resolution of ~5 s. Figures 3b–3g show that the pitch angle distributions evolved from a $\sin^N(\alpha)$-type distribution to one sharply peaked (FWHM ~ 16°) near 75°, for this flux burst. The electron fluxes $<60°$ ($>120°$) and 90° remained essentially unchanged while the fluxes near 75° increased by factors of 4 to 5. Figures 3g–3j show the pitch angle distributions returning to their preburst form. Such evolution of the pitch angle distributions occurred during all the flux bursts observed between 0835 and 0905 UT in Figure 2.

The EMFISIS BM data are summarized in Figure 4 where Figure 4a shows a frequency-time spectrogram of the waveform data obtained by performing FFTs on the waveform data. The black lines in Figure 4 identify half the electron cyclotron frequency ($f_{ce}/2$) that separates the lower band (LB) and upper band (UB) chorus. The LB was relatively stable in bandwidth from 0901:30 to 0901:49 where it disappears. It occurs again after 0901:57 but broader in frequency range. Initially, the UB chorus was in a relatively narrow frequency band, until ~0901:42, then became broader with a third higher-frequency band occurring near 0901:46–:53 UT. The UB band then remained relatively broad for the rest of BM interval. Individual chorus risers are clearly observed in these waveform data with peak wave amplitudes of a few $\times 10^{-4}$ nT^2/Hz.

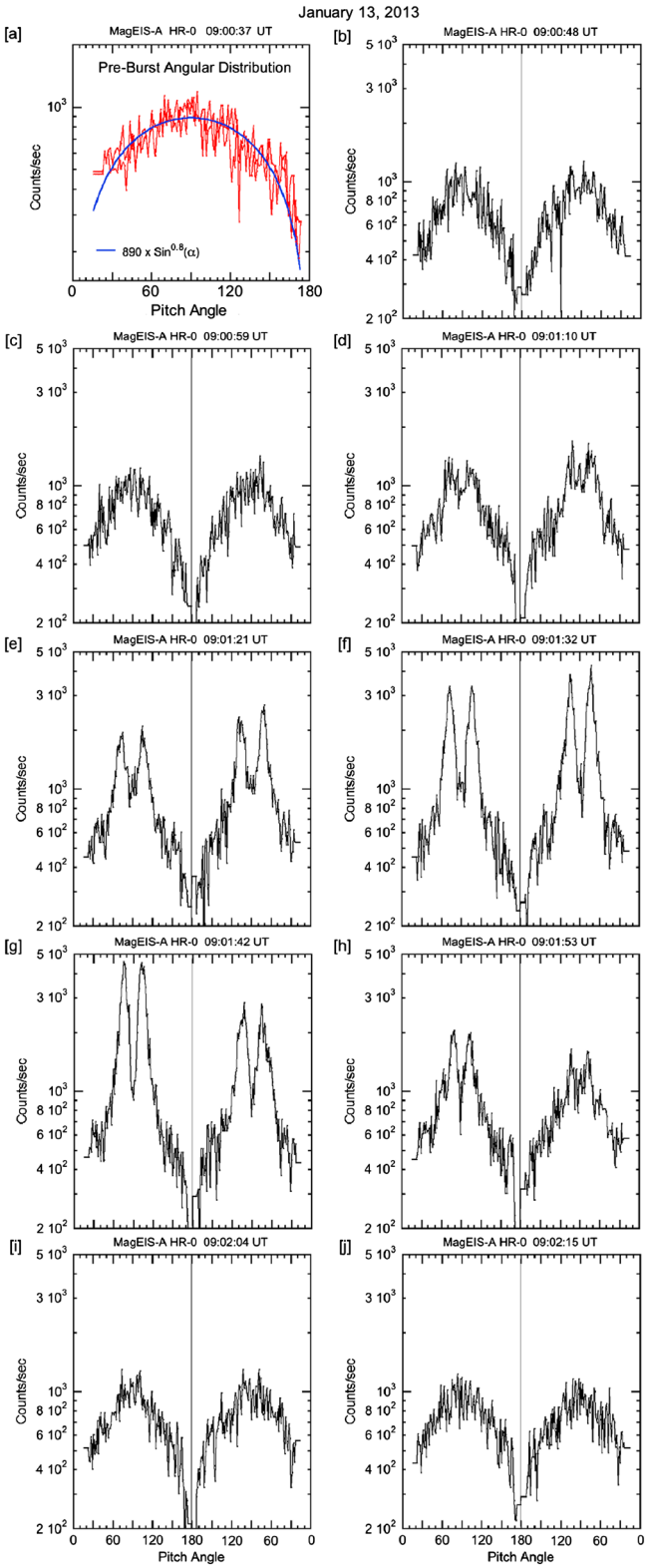

Figure 3. High-resolution electron pitch angle distributions taken during the flux burst near 0901:40 UT in Figure 2. (a) The fit to a preburst angular distribution that is plotted on 0–180° horizontal scale and combines two half spins together. (b–j) The evolution of angular distributions through the flux burst, spanning roughly 2 min. Each of these latter panels includes data from a full satellite spin with the vertical line separating the two halves of a spin into pitch angles 0–180° and 180–0°.

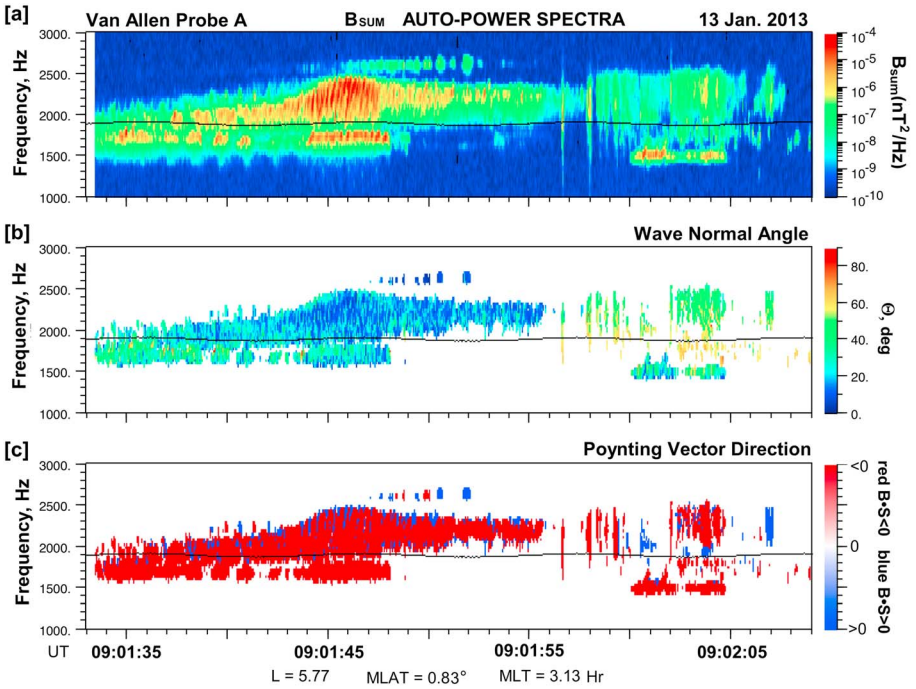

Figure 4. EMFISIS burst waveform data showing (a) chorus elements plus (b) wave normal angle, and (c) Poynting vector direction for the flux and chorus burst near 09:01:40 UT.

Figure 4 also shows the wave normal angle (Figure 4b) and Poynting vector direction (Figure 4c) relative to B. These indicate that the chorus emissions were propagating roughly antiparallel to the magnetic field direction. During the time of the most intense UB chorus in Figure 4a the wave normal angle was ≤20° relative to B. During the early and late part of the BM interval the wave normal angle was more oblique (40–50°). It is during these latter times that the electron pitch angle distributions were more like $\sin^N(\alpha)$ while the interval where the wave normal angle was ≤20° coincides with the strong enhancement in the electron fluxes at $\alpha \sim 75°$ (105°, etc.) as shown in Figure 3.

One can use the particle and wave data in Figures 2–4 and a measure of the plasma density to estimate the electron resonance energy. The upper hybrid line from the EMFISIS HFR spectra (not shown) was used to estimate the plasma density. This line was at ~19.5 kHz, during the flux burst near 0902 UT in Figure 2, from which we infer a density of ~4.5 cm^{-3}. The f_{ce} was ~3.75 kHz, UB chorus was 1.9–2.3 kHz, and the LB chorus was ~1.65–1.8 kHz (see Figure 4). Combining these, an estimate of the parallel resonance energy for the electrons is ~1.04–2.3 keV for UB chorus and ~2.9–3.9 keV for LB chorus. The peak flux in the flux burst occurred near 0902 UT at a local pitch angle of ~75°. Folding this into the estimate gives a range of total electron energies of ~15–35 keV for resonance with UB chorus and ~42–59 keV for LB chorus. Neither MagEIS-A LOW nor HOPE-A observed a flux burst response in electrons <17 keV or > 30 keV. The resonance energy estimates for UB chorus are consistent with the MagEIS-A LOW HR0 energy response. They are also consistent with the electron energies at which flux bursts were observed by HOPE-A (≥15 and <30 keV, see supporting information). We note that as the UB chorus broadened upward in frequency, the lower bound of the resonance energy range would be expected to decrease. In any case, the electron observations did not show a significant response for energies <17 keV.

4. Discussion

Questions about the correlated electron and wave features of this event fall into two categories. Do the chorus waves alter the electron velocity distributions to form the observed angular peaks? Does the free energy in the electron distributions generate the wave emissions through some instability? Or, is it some combination of these and other possibilities? In any case, the source of the particles comprising the off-equatorial pitch angle peaks must also be explained.

The observed electron angular distributions in the flux bursts resemble a ring distribution. Such distributions provide a positive gradient parallel and perpendicular relative to the magnetic field. *Umeda et al*. [2007, 2012] showed that electromagnetic chorus and electron cyclotron harmonic (ECH) waves could be generated by such distributions. Model chorus waves, for example, were unstable in two relatively narrow bands above and below $f_{ce}/2$, similar to the observed frequency spectra in Figures 2 and 4. However, those simulations had ring distributions with zero parallel velocity in contrast to the substantial parallel velocities inferred from Figure 3. ECH emissions were observed during the study interval (not shown), but they had no variations that correlate with the bursts of chorus emission or electron fluxes.

Many questions are still left unanswered. There is no obvious explanation for the quasiperiodic nature of the bursts of electrons and simultaneous chorus emissions. One can speculate that some aspect of the wave-particle interaction was turning the electromagnetic part of the instability on and off. For example, *Umeda et al*. [2007] showed that it was possible to shift the wave growth from the whistler mode instability to the electrostatic ECH instability by adjusting the parameters of a ring distribution. The chorus wave fields could also accelerate or scatter the electrons to generate, parasitically, the peaks in the electron pitch angle distributions.

One possibility for generating the bursts is that part of the higher electron flux at lower energies was accelerated. We note that the electron energy spectra had a steep flux versus energy gradient (see supporting information) for $10 < \mathrm{Ee} < 40$ keV ($\mathrm{J} \sim \mathrm{E}^{-6.1}$) while the spectral shape was much less steep below 10 keV ($\mathrm{J} \sim \mathrm{E}^{-0.86}$), indicating that the spacecraft was near a 10 keV Alfvén boundary [*Ejiri*, 1978]. Transfer of parallel energy to electrons from the lower energy part of the steeply falling spectrum could give rise to both an off 90° peak and flux enhancements. *Tao et al*. [2012] used both quasi-linear and nonlinear theory to produce pitch angle and energy diffusion rates due to chorus waves. The resulting model diffusion rates were dependent on the wave bandwidth and amplitude. However, the diffusion rates were determined for waves with frequencies $< f_{ce}/2$. As we showed above, the resonance conditions for the bursts best match waves with frequencies $> f_{ce}/2$. To infer whether energy and pitch angle diffusion can explain the observations, one needs an assessment like that of *Tao et al*. [2012] for waves with frequencies $> f_{ce}/2$. As can be seen in Figure 2, the peak wave amplitudes of the chorus bursts at $> f_{ce}/2$ were mostly in the range of 10^{-6} to 10^{-5} $\mathrm{nT}^2/\mathrm{Hz}$. The waves amplitudes at $< f_{ce}/2$ were roughly 10% of those $> f_{ce}/2$. Comparing the observed wave amplitudes and bandwidths shown in Figure 4 indicates linear theory may be on the cusp of nonapplicability [*Tao et al*., 2012]. In any case, the narrow-observed peaks in the pitch angle distributions are not likely the result of a diffusive process that tends to smear out such structure. It is clear that an event-specific simulation based on the observations may need to be done to come to firm conclusions.

As was also mentioned above, MagEIS-B and HOPE-B (MagEIS-B shown in the supporting information, HOPE-B not shown) also observed the flux bursts. It was found that if one shifted the MagEIS-A flux bursts 127 s forward in time relative to the MagEIS-B flux bursts, there was a good match between the A and B flux bursts (see supporting information). Why would this be? Probe A is trailing probe B in L and parallel to it but at an earlier MLT by ~0.3 h. Both spacecraft are postmidnight near 3 MLT. Does this mean that the satellites are crossing regions of chorus and flux burst activity with B leading A or is it possible that the 127 s represents the time for the particles to propagate from one spacecraft to the other? It cannot be a simple gradient-curvature drift time because the A offset is the wrong sign for that since the bursts at B would have to arrive later than at A; but the reverse was observed.

As noted above, Probe A was at a 10 keV Alfvén boundary. Thus, it is possible that fluctuations in the large-scale electric field could alternately put the 17–25 keV electrons onto trajectories that do then do not intercept the satellites sporadically. Thus, small changes in the electric field could change the access, or lack thereof, that 17–25 keV electrons have to the Van Allen probes. To better examine how the 127 s difference could occur requires modeling the conditions using a tool such as RCM-E (Rice Convection Model - Equilibrium) [*Lemon et al*., 2004] to examine the plasma and particle motions, which is outside the scope of this publication but is being considered as part of a larger study.

Acknowledgments

This work was supported by Van Allen Probes ECT funding provided by JHU/APL contract 967399 and EMFISIS funding provided by JHU/APL contract 921647, both under NASA's Prime contract NAS5-01072. Work at Los Alamos National Laboratory was performed under the auspices of the United States Department of Energy under Interagency Purchase Request NNG07EK09I. Work at JHU/APL was supported by NASA grant NNX10AK93G. The OMNI data (*SYM-H*) were obtained from the GSFC/SPDF OMNIWeb interface at http://omniweb.gsfc.nasa.gov, and the *AE* data were obtained from the WDC for Geomagnetism, Kyoto, at http://swdcwww.kugi.kyoto-u.ac.jp/ae_provisional/index.html.

The Editor thanks two anonymous reviewers for assistance evaluating this paper.

References

Blake, J. B., et al. (2013), The Magnetic Electron Ion Spectrometer (MagEIS) instruments aboard the Radiation Belt Storm Probes (RBSP) spacecraft, *Space Sci. Rev.*, *179*, 383–421, doi:10.1007/s11214-013-9991-8.

Ejiri, M. (1978), Trajectory traces of charged particles in the magnetosphere, *J. Geophys. Res.*, *83*, 4798–4810, doi:10.1029/JA083iA10p04798.

Funsten, H. O., et al. (2013), Helium, Oxygen, Proton, and Electron (HOPE) mass spectrometer for the Radiation Belt Storm Probes mission, *Space Sci. Rev.*, *179*, 423–484, doi:10.1007/s11214-013-9968-7.

Kletzing, C. A., et al. (2013), The Electric and Magnetic Field Instrument Suite and Integrated Science (EMFISIS) on RBSP, *Space Sci. Rev.*, *179*, 127–181, doi:10.1007/s11214-013-9993-6.

Lemon, C., R. A. Wolf, T. W. Hill, S. Sazykin, R. W. Spiro, F. R. Toffoletto, J. Birn, and M. Hesse (2004), Magnetic storm ring current injection modeled with the Rice Convection Model and a self-consistent magnetic field, *Geophys. Res. Lett.*, *31*, L21801, doi:10.1029/2004GL020914.

McIlwain, C. E. (1961), Coordinates for mapping the distribution of magnetically trapped particles, *J. Geophys. Res.*, *66*(11), 3681–3691, doi:10.1029/JZ066i011.

Mauk, B. H., N. J. Fox, S. G. Kanekal, R. L. Kessel, D. G. Sibeck, and A. Ukhorskiy (2013), Science objectives and rationale for the Radiation Belt Storm Probes mission, *Space Sci. Rev.*, *179*, 3–27, doi:10.1007/s11214-012-9908-y.

Millan, R. M., and the Balloon Array for Radiation Belt Relativistic Electron Losses (BARREL) Team (2011), Understanding relativistic electron losses with BARREL, *J. Atmos. Sol. Terr. Phys.*, *73*, 1425–1434, doi:10.1016/j.jastp.2011.01.006.

Spence, H. E., et al. (2013), Science goals and overview of the Energetic Particle, Composition, and Thermal plasma (ECT) suite on NASA's Radiation Belt Storm Probes (RBSP) mission, *Space Sci. Rev.*, *179*, 311–336, doi:10.1007/s11214-013-0007-5.

Tao, X., J. Bortnik, J. M. Albert, and R. M. Thorne (2012), Comparison of bounce-averaged quasi-linear diffusion coefficients for parallel propagating whistler mode waves with test particle simulations, *J. Geophys. Res.*, *117*, A10205, doi:10.1029/2012JA017931.

Tsyganenko, N. A. (1989), A magnetospheric magnetic field model with a warped tail current sheet, *Planet. Space Sci.*, *37*, 5–20, doi:10.1016/0032-0633(89)90066-4.

Umeda, T., M. Ashour-Abdalla, D. Schriver, R. L. Richard, and F. V. Coroniti (2007), Particle-in-cell simulation of Maxwellian ring velocity distribution, *J. Geophys. Res.*, *112*, A04212, doi:10.1029/2006JA012124.

Umeda, T., S. Matsukiyo, T. Amano, and Y. Miyoshi (2012), A numerical electromagnetic linear dispersion relation for Maxwellian ring-beam velocity distributions, *Phys. Plasmas*, *19*, 072107, doi:10.1063/1.4736848.

Wygant, J. R., et al. (2013), The Electric Field and Waves Instrument on the Radiation Belt Storm Probes mission, *Space Sci. Rev.*, *179*, 183–220, doi:10.1007/s11214-013-0013-7.